AUT Journal of Mechanical Engineering

AUT J. Mech. Eng., 1(1) (2017) 49-54
DOI: 10.22060/mej.2016.782

Investigation of Effective Parameters on a Thermal Load in a Thermo-Acoustic Refrigerator

A. Mohammadi, S. M. A. Alavi*

Mechanical Engineering Department, Mashhad Branch, Islamic Azad University, Mashhad, Iran

ABSTRACT: This article aims to investigate the effects of various parameters on the thermal load. The governing equations include continuity and Navier-Stokes equations for the flow field and the energy equation for the temperature distribution in transient mode. Numerical simulation of the thermo-acoustic refrigerator by taking the non-zero thickness of the plate stack into account, that is a conjugate heat transfer problem, in a form of 2D has been performed in FLUENT software. Real simulation of thermoacoustic refrigerators needs a consideration of both heat exchangers, whereas in most simulations one or both heat exchangers have been neglected. Results are influenced by the steady state. Input dynamic pressure should be adjusted according to the temperature of the heat exchanger. The results demonstrate the effect of the distance of the plates on the average thermal load suggesting that the distance between the plates should be four times of the thickness of the plates so that the device works properly. By increasing the distance of the plates thermal load decreases. This is mainly because of pressure amplitude reduction induced by an increase in the distance between the plates.

Review History:

Received: 10 June 2016
Revised: 7 October 2016
Accepted: 24 October 2016
Available Online: 8 November 2016

Keywords:

Refrigerator
Thermo-acoustic
Distance
Plate stack
Thermal load

1- Introduction

Thermoacoustic refrigerators are devices that use sound to produce cooling. They mainly include an audio source (speaker) connected to a resonator formed by the gas-filled. In resonator, a stack consisting of two parallel plates and a heat exchanger is installed (Fig. 1) [1]. One of the most important advantages of such systems is that heat losses such as industrial and household losses or solar energy instead of fossil fuels for power generation can be exploited. On the other hand, in these systems, there are no moving parts resulting in minimized vibration and lubrication. Their maintenance is very easy and inexpensive. In addition, the fluid used in thermo-acoustic systems such as helium and air has capabilities such as non-flammability and non-toxicity. It should be noted that these systems also have problems; the most important ones are low power and efficiency [2]. Recently, several numerical solutions for modeling the flow field have been presented in the refrigerator for thermo-acoustic. Cao et al. [3] carried out the first thermo-acoustic simulation with more than one dimension. They have defined a useful quantity of energy flux density used to transfer energy in a thermo-acoustic phenomenon. In their study, a constant temperature stack of zero thickness is simulated and the results are compared with the analytical solution. Ishikawa and Mee's research [4] was, in fact, the extension of that of Cao et al. [3]. Using both long and short stacks, they studied the energy-flux density, particle trajectory and the rate of entropy generation. Piccolo and Pistone [5] calculated heat transfer coefficient in an oscillatory flow for a thermo-acoustic device. Then, they studied how to change the heat transfer between the stack and gas by changing parameters such as plates distance and the amplitude of the sound. The results showed that the net transferred energy exchanges in a small area from the edge of the stack. The range is a function of the distance between the plates and after a specified interval; it has a fixed values, independent of the distance. Tasnim and Frazer [6] did a numerical simulation of the flow and temperature fields in a thermoacoustic refrigerator. Also, solved the energy equation for a stack, hence they studied a conjugate heat transfer problem. In this paper, the boundary conditions by assuming the standing wave have been more clearly described. Piccolo [7] modeled heat exchangers in a thermo-acoustic refrigerator and used theoretical analysis of linear equations. Then, he studied the effect of the geometry of the heat exchangers and the device working conditions. After that, he worked on heat transfer in the heat exchanger and then the optimal blade length of heat exchanger and the distance between them. At the end, he concluded that the heat exchanger length in the optimal case should be less than the peak-to-peak displacement distance of a gas element. This is because higher quantities have a small effect on increasing efficiency and they increase losses .He put the distance between the heat exchanger fins, at least twice and up to four times the thermal penetration depth to achieve a good performance. Namdar et al. [8] did a numerical investigation of the thermoacoustic refrigerator at weak and large amplitudes considering cooling effect.

Given that the previous researchers did not mention the influence of parameters affecting the thermal load, in the present study, we aim to investigate the effect of parameters such as plates distance, amplitudes of inlet pressure and heat exchangers' temperature on device' thermal load. Simulation of the thermoacoustic refrigerator in a two-dimensional way is performed.

Corresponding author, E-mail: m-a-alavi@mshdiau.ac.ir

2- Governing Equations

The governing equations, including continuity, momentum, and transient energy equations are as follows:

Continuity equation:

$$\frac{\partial \rho}{\partial t} + \nabla.(\rho u) = 0 \tag{1}$$

Momentum equation:

$$\frac{\partial \rho u}{\partial t} + \nabla.(\rho u u) = -\frac{\partial P}{\partial x} + \nabla.\mu \nabla u + S_{mx} \tag{2}$$

$$\frac{\partial \rho v}{\partial t} + \nabla.(\rho u v) = -\frac{\partial P}{\partial y} + \nabla.\mu \nabla v + S_{my} \tag{3}$$

and energy equation:

$$\frac{\partial \rho h_0}{\partial t} + \nabla.(\rho h u) = \nabla.k \nabla T + S_h \tag{4}$$

where h_o and h are defined as follows:

$$h_0 = h + \frac{1}{2}(u^2 + v^2) \tag{5}$$

$$h = C_p(T - T_m) \tag{6}$$

In this equation, ρ is the density, u and v demonstrate the velocities in the x and y directions, S is the thermal source, P is the pressure, T is the temperature and μ is the dynamic viscosity.

The energy equation in the stack will also be solved, which represents the conjugate heat transfer [9].

$$\frac{\partial \rho C_p T}{\partial t} = \nabla.k \nabla T \tag{7}$$

where C_p is specific heat at constant pressure and k is the thermal conductivity, depending on temperature, as the following formulas:

$$\mu = \mu_m (\frac{T}{T_m})^b \tag{8}$$

$$k = k_m (\frac{T}{T_m})^b \tag{9}$$

The subscript m means that the properties are derived at the average temperature. The parameter b equals to 0.667. The working fluid is air and assumed as ideal gas [8].

3- Numerical Method and Boundary Conditions

The commercial software Fluent is used for simulations. The QUICK scheme is used for discretization of the convective and diffusive terms and the second-order fully implicit scheme is employed for the discretization of the temporal term [10]. The PISO algorithm is exploited in order to make a connection between the pressure and velocity fields [11]. Computational domain is demonstrated in Fig. 1.

Table 1 lists the parameters and properties presented in mean temperature.

Upper and lower boundary conditions are symmetrical:

$$v = 0., \frac{\partial u}{\partial y} = 0., \frac{\partial P}{\partial y} = 0., \frac{\partial T}{\partial y} = 0. \tag{10}$$

Constant temperature boundary condition in heat exchangers and conjugate heat transfer boundary condition in the stack are considered:

$$T_{solid} = T_{fluid}, k_{solid} \frac{\partial T_{solid}}{\partial x} = k_{fluid} \frac{\partial T_{fluid}}{\partial x} \tag{11}$$

Velocity and pressure boundary conditions on the stack and heat exchanger according to Eq. (12) are considered.

$$v = 0., u = 0., \frac{\partial P}{\partial y} = 0. \tag{12}$$

The left side refrigerator inlet pressure boundary condition is considered to be as follows

$$P = P_m + Re\{P_1 e^{i\omega t}\} \tag{13}$$

where P_m is the average pressure, Re {} represents the real sector of oscillating pressure amplitude in the standing wave, ω represents the angular frequency $\omega = 2\pi f$ and f is the frequency. P_1 for an ideal wave is as follows:

$$P_1 = P_A \cos(kx) \tag{14}$$

where P_A is the amplitude of the sound wave pressure. $k=2\pi\lambda$ wave number and λ is the wavelength. The right side refrigerator wall boundary condition is as follows:

$$v = 0., \frac{\partial u}{\partial y} = 0., \frac{\partial P}{\partial x} = 0., \frac{\partial T}{\partial x} = 0. \tag{15}$$

The initial value of pressure, temperature and speed are

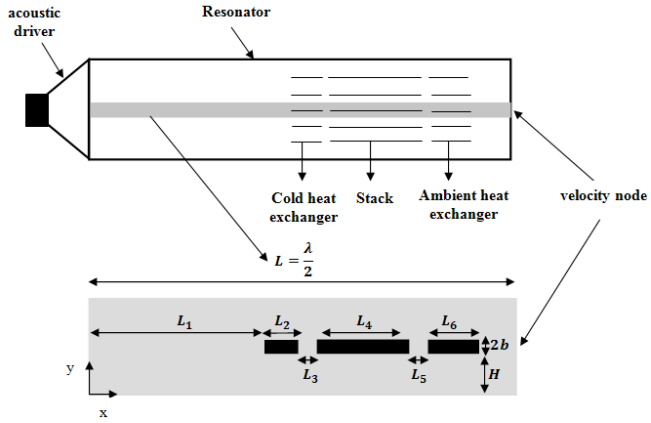

Fig. 1. Thermoacoustic refrigerator and computational domain

Table 1. List of parameters and properties

Parameter	Unit	Value
$C_{p,fluid}$	J/kg.K	1007
k_{fluid}	W/m.K	0.0261
μ_{fluid}	N.s/m^2	0.18385×10^{-4}
$C_{p,solid}$	J/kg.K	840
k_{solid}	W/m.K	1.05
ρ_{solid}	kg/m^3	2600
a	m/s	347.2
f	1/s	200
$k = 2\pi/\lambda$	1/m	3.619
$\lambda=a/f$	m	1.736
$2b$	m	0.0002
L	m	0.868
L_1	m	0.7108
L_2	m	0.005
L_3	m	0.0002
L_4	m	0.07
L_5	m	0.0002
L_6	m	0.01

P_m, T_m and zero, respectively. The initial temperature is the average temperature of the hot and cold heat exchangers. The sound wave of the pressure amplitude after passing through the heat exchanger and stack hits the end wall and returns. Then interferes with other waves, that results in generating a standing wave. Reynolds number is calculated according to Eq. (16), it is less than 400, therefore laminar flow is considered.

$$Re = \frac{2u_{max}}{\sqrt{\mu\omega/\rho}} = 35 \quad (16)$$

where $u_{max} = P_A/\rho_m a$, in which a represents the speed of sound [12]. Wave amplitude in the x-direction is half of the wavelength. Fig. 2 shows a part of the network stack area. Studies of the network size have been performed on the heat load. The cell size in the x-direction and in the y-direction is equal to $\Delta x = 0.0025\lambda$ and $\Delta y = 0.05h$, respectively.

Energy flux density in the y-direction, the drive ratio, and blockage ratio are calculated from the following relations.

$$\dot{e} = \rho v\left(\frac{1}{2}v^2 + h_1\right) - k\frac{\partial T}{\partial y} \quad (17)$$

$$\mathrm{DR} = \frac{P_A}{P_m} \quad (18)$$

$$\mathrm{B}_r = \frac{\mathrm{H}}{\mathrm{H}+\mathrm{h}} \quad (19)$$

where

$$V = \sqrt{(u^2 + v^2 + w^{2)}} \quad (20)$$

H is half the distance between the plates and b is half the thickness of the plates. To obtain an average over time for each parameter during a cycle, the following formula is used:

$$\bar{z} = \frac{\omega}{2\pi}\int_0^{\frac{2\pi}{\omega}} \dot{z}dt \quad (21)$$

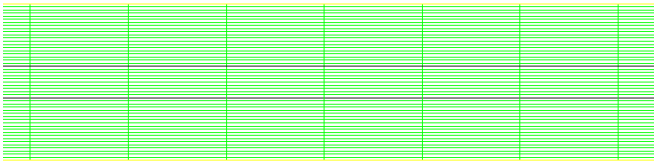

Fig. 2. Two-dimensional networks in the stack

4- Results

4- 1- Validation

Energy flux density in simulations is compared with that of the results of Namdar et al. study [8]. The amount of energy crossing the surface unit per time is illustrated by ėy and the graph over the plate stack is drawn. Energy mainly enters or exits at the edges but in the middle of the plate, the amount of energy that enters is as the amount that leaves. Therefore, the energy average on the length of the cycle plate is zero and Fig. 3 shows a suitable match.

4- 2- The effect of blockage ratio

Fig. 4 shows the effect of blockage ratio Br on the average thermal load that is drawn by DR=5% and $T_c/T_h = 0.99$ and with a constant thickness of the plates of stack and heat exchangers. As shown in the Fig. 4, at $Br < 0.72$, the device is unable to absorb heat from the cold heat exchanger. On the contrary, the heat is transferred to the cold heat exchanger, since $Q_c < 0$ because of increasing heat losses due to the small

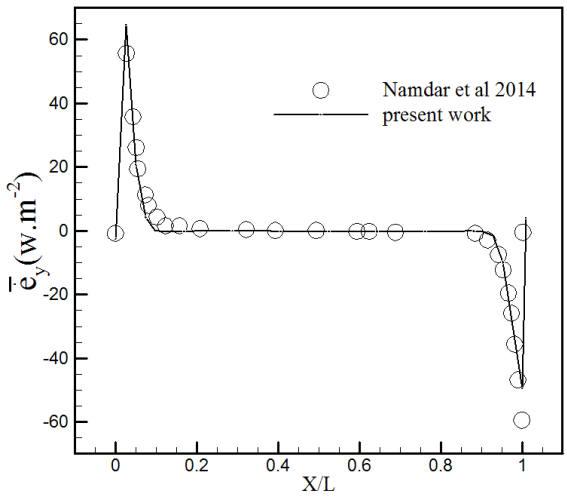

Fig. 3. Energy flux density over the stack plate compared to Namdar et al. results [8]

plates distance. At $0.72 < Br < 0.78$ no heat is exchanged between the cold heat exchanger and the device. At $Br > 0.78$, the device absorbs heat from the cold heat exchanger. The thermal load declines at $Br > 0.6$ because $Q_h > 0$. To enable the device to transmit heat to the hot heat exchanger, we should have $Br > 0.6$. The best mode for the device to operate successfully should be $Br = 0.8$ and according to Eq. (19), plates distance must be four times the thickness of the plates. Fig. 5 shows the effect of dimensionless ratio H/δ_v on the average heat load. δ_v is the thickness of the viscous boundary layer and is calculated by Eq. (22).

$$\delta_v = \sqrt{\frac{2\mu}{\rho\omega}} \quad (22)$$

As can be seen in the figure, for the device to work properly, $H/\delta_v = 2.5$ should be obtained.

4- 3- The effect of drive ratio and the temperature ratio of the heat exchanger

Fig. 6 shows the effect of drive ratio on the average heat load by taking the temperature of the cold heat exchanger to the temperature of the hot heat exchanger by 0.99 during a cycle. It was found that by DR<2.3% the device could not absorb

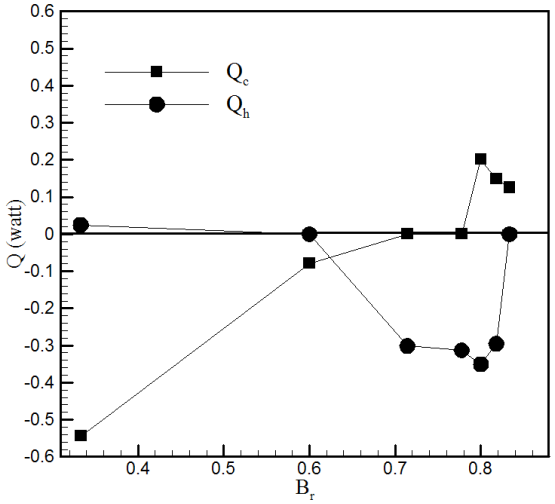

Fig. 4. The effect of blockage ratio on the average heat load

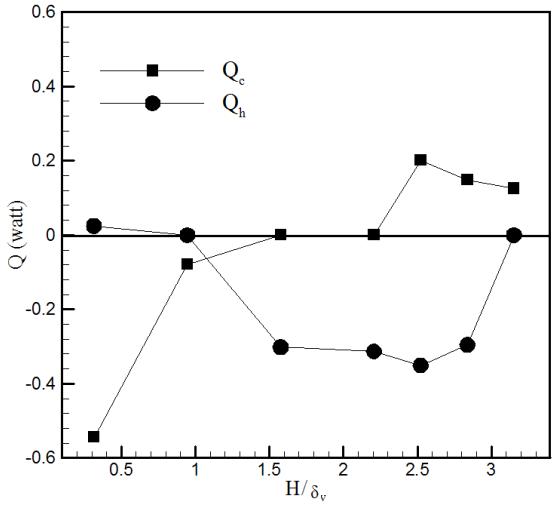

Fig. 5. The effect of non-dimensional ratio H/δ_v on the average heat load

heat from the cold heat exchanger. Instead, heat is transferred to the cold heat exchanger because of $Q_c<0$ condition. Therefore, it can be understood that by $DR<19\%$, the device could not absorb heat from the cold heat exchanger. Instead, heat is transferred to the hot heat exchanger and the device absorbs heat from the heat exchanger because of $Q_h>0$ condition. The low pressure range explains the reason for this phenomenon. In addition, the amount of heat transferred to the hot heat exchanger, should be higher than that of the cold heat exchanger. This is because the coefficient of performance of thermo acoustic refrigerator should always be positive.

$$\mathrm{COP}=\frac{Q_c}{|Q_h|-Q_c}\Rightarrow|Q_h|>Q_c\Rightarrow COP>0 \tag{23}$$

Since the device is able to work properly, it must be $DR > 2.3\%$.

Fig. 7 shows the effect of the drive ratio on the average heat load of the $T_c/T_h=0.95$ during a cycle. For $DR < 19\%$, the device cannot absorb heat from the cold heat exchanger. Instead, it transfers the heat to the cold heat exchanger ($Q_c < 0$). In $DR< 5\%$, the device cannot transmit heat to the hot heat exchanger, as well. On the contrary, it absorbs heat from the heat exchanger ($Q_h > 0$). For this reason, the device is able to work properly by $DR>19\%$. The conclusion from this

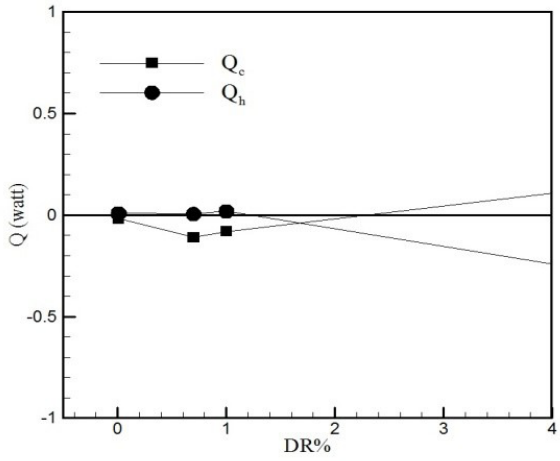

Fig. 6. The effect of drive ratio on the average heat load by $T_c/T_h=0.99$

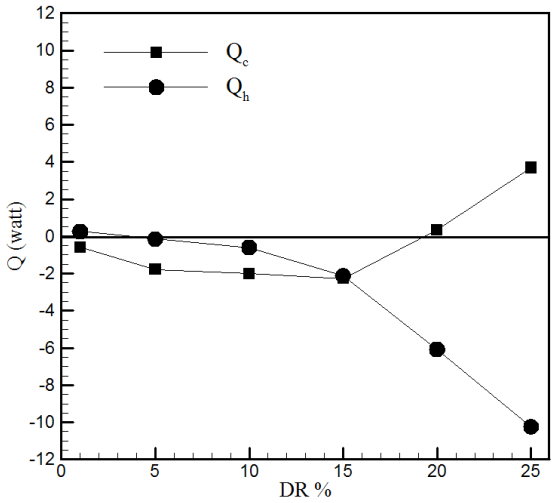

Fig. 7. The effect of the drive ratio on the average heat load by $T_c/T_h=0.95$

section is that the input dynamic pressure should be properly adjusted according to the temperature of the heat exchangers so that the device works properly. Time to reach steady state condition, in this case should be twice at $T_c/T_h= 0.99$.

4- 4- The effect of displacement on gas element

Displacement of the gas element is calculated as follows:

$$\delta=\frac{2u_{\max}}{\omega} \tag{24}$$

where u_{max} is the speed amplitude and is concerned with the pressure, and ω is the angular frequency. With a constant frequency, speed amplitude varies with pressure amplitude and they are interconnected by the following equation:

$$u_{\max}=\frac{P_A}{\rho_m a} \tag{25}$$

For the frequency of 200 Hz and amplitude pressure of 1 kPa, the speed is 2.5 m/s. Thus, displacement obtained from gas elements is equal to:

$$\delta=\frac{2\times2.5}{2\pi\times200}=0.0039m$$

For amplitude pressure of 15 kPa and speed of 37.25 m/s. the displacement of the gas element is equal to:

$$\delta=\frac{2\times37.25}{2\pi\times200}=0.059m$$

For amplitude pressure of 1 kPa, the displacement of the gas element is less than the length of heat exchangers. As shown in Fig. 8, the temperature of the cold heat exchanger is marked in blue and temperature of the warm heat exchanger in red in the middle of the heat exchanger, the average temperature of the gas element in a cycle equals to the temperature of the heat exchanger. As a result, heat transfer is zero and on side of the heat exchanger, the gas element temperature is higher than that of the heat exchanger and on the other side, the gas element temperature is lower than that of the heat exchanger and on the left and the right sides, the temperature of the gas element increases.

For amplitude pressure of 15 kPa, the displacement of the gas element is more than the length of heat exchangers. As seen in Fig. 9, in cold heat exchanger, the average temperature of the gas element is less than that of the cold heat exchanger.

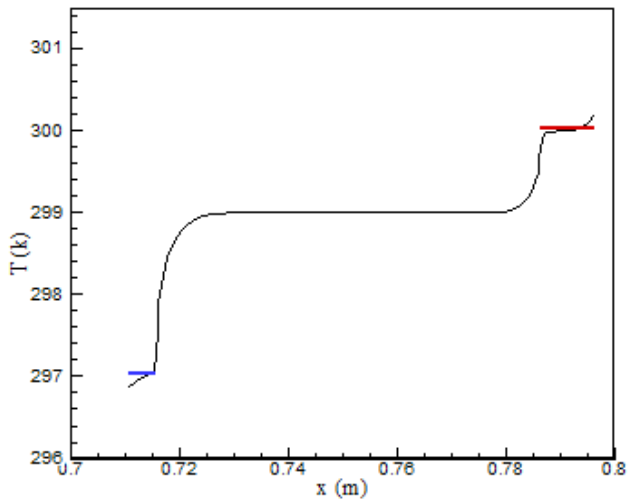

Fig. 8. Average temperature gas element y = 0.00061m, P_A = 1 kPa

As a result, the heat from the cold heat exchanger transmits to the gas element and in the hot heat exchanger, the average temperature in the gas element is higher than that of hot heat exchanger. Consequently, the heat from gas element transmits to the hot heat exchanger. Therefore, it can be concluded that the length of the displacement of gas elements is greater than that of the heat exchanger until the heat transfer between the heat exchanger and gas elements is fully taken.

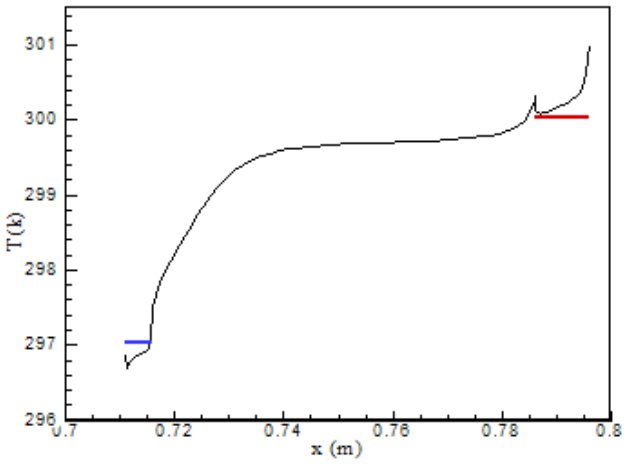

Fig. 9. Average temperature gas element y = 0.00061m, P_A = 15 kPa

Fig. 10 shows the contour of temperature in the thermo-acoustic refrigerator during one cycle with pressure amplitude of 1 kPa and the temperature of the cold heat exchanger of 297 K and the temperature of the hot heat exchanger of 300 K. To see the changes during a cycle, thermoacoustic refrigerator have been divided into ten parts. Fig. 10(a) shows the beginning of the cycle. The gas element on the left, that is a cold heat exchanger, is considered. At this time, gas element temperature is lower than the temperature of cold heat exchanger. Thus, it takes a little heat from the cold heat exchanger. Next, as shown in Fig. 10(b), gas moves to the right and to the left and the temperature of the gas elements increases on both sides. As shown in Fig. 10(d), the pressure is maximum and the gas element temperature is higher than that of the hot heat exchanger. Therefore, little heat is transferred to the warm heat exchanger. In Fig. 10(e), gas moves to the left, the temperature of the gas elements decreases on both sides. In Fig. 10(g), the gas element again reaches the cold heat exchanger and the cycle resumes. According to the refrigeration cycle, in which normally after each compression stroke, the fluid is cooled and after each expansion stage, it is heated; we can see that most heat absorption is from the cold heat exchanger at the beginning of the cycle (after the compression stroke).

The highest heat transferred to the warm heat exchanger is in the middle-of-cycle (after the expansion process). During this cycle, the heat from the cold source is transferred to the heat source.

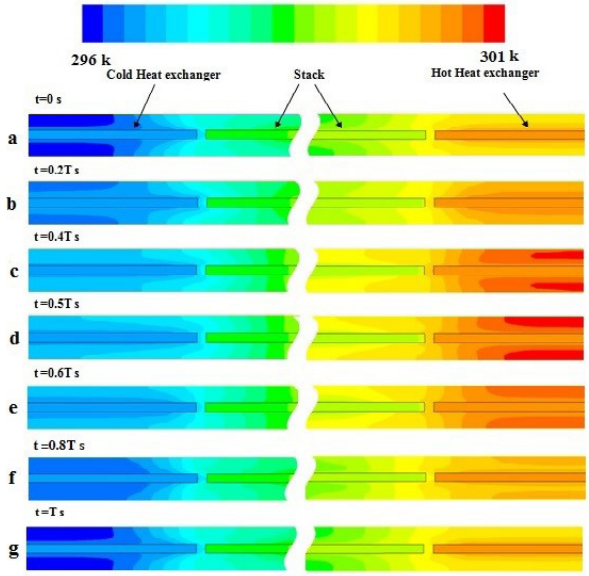

Fig. 10. Temperature contour during one cycle

5- Conclusion

Real simulation of thermoacoustic refrigerators needs a consideration of both heat exchangers, whereas in most simulations one or both heat exchangers are neglected. In this study, the first survey was conducted on the distance between the plates on the thermal load. Because the coefficient of performance of refrigerator depends on that. Also, the amount of heat absorbed and excreted determines the coefficient of performance of the refrigerator. Results are influenced by the steady state condition. To make the device capable of working successfully, either the distance between the plates should be four times of their thickness or the distance between the plates should be 2.5 times of the thickness of the viscous boundary layer. On the one hand, input dynamic pressure should be adjusted according to the temperature of the heat exchanger, and on the other hand, the gas element temperature should be lower than the temperature of the heat exchanger. The temperature difference between heat exchangers, at any increasing rate should be selected as a higher input dynamic pressure until the device works properly. Time to steady state at a high-temperature difference between the heat exchanger is longer. The length of the displacement of gas elements should be longer than the length of the heat exchanger until heat transfer between the heat exchanger and gas elements are fully taken. As a result, in heat exchangers, heat enters

from one side and exits from the other.

List of Symbols

a	Speed of sound, m/s
b	Half the distance between the plates, m
Br	Blockage ratio
COP	Refrigerator performance coefficient
C_p	Specific heat capacity, J/kg.K
DR	Drive ratio
e	Energy
f	Frequency, 1/s
H	Half the distance between the plates, m
h	Energy, kJ/kg
k	Thermal conductivity, W/m.K
L	Length, m
P	Pressure, Pa
Q	Heat, kJ
u	Speed in the direction of x, m/s
S	Thermal source
T	Temperature, K
V	Velocity, m/s
v	Speed in the direction y, m/s
w	Speed in the direction of z, m/s

Symptoms Greek

ρ	Density, kg/m^3
μ	Dynamic viscosity, kg/m.s
δ	Displacement elements, m
λ	Wavelength, m
ω	Angular frequency, rad/s

Subtitle

c	Cold
f	Fluid
h	Hot
m	Average
s	Solid

References

[1] G.W. Swift, Thermo-acoustic engines, *J. Acoust. Soc.*, 84 (1998) 1146-1152.

[2] G.W. Swift, Thermo-acoustics: a unifying perspective for some engines and refrigerators, *Fifth draft*, 2001.

[3] J.R.O. N. Cao, G. W. Swift, Energy Flux Density in a Thermo-acoustic Couple, *J. Acoust*, 99 (1996).

[4] D.M. H. Ishikawa, Numerical Investigations of Flow and Energy Fields near a Thermo-acoustic Couple, *J. Acoust. Soc.*, 111 (2002) 831-839.

[5] G.P. A. Piccolo, Estimation of heat transfer coefficients in oscillating flows: The thermoacoustic case, *International Journal of Heat Mass Transfer*, 49 (2006) 1631-1642.

[6] R.A.F. S. H. Tasnim, Computation of the flow and thermal fields in a thermos-acoustic refrigerator, *International Journal of Heat Mass Transfer*, 37 (2010) 748-755.

[7] A. Piccolo, Numerical computation for parallel plate thermo-acoustic heat exchangers in standing wave oscillatory flow, *International Journal of Heat and Mass Transfer*, 54 (2011) 4518– 4530.

[8] A.K. A. Namdar, E. Roohi, Numerical Investigation of Thermo-acoustic Refrigerator at Weak and Large Amplitudes Considering Cooling Effect, *Cryogenics*, 67 (2014) 36-44.

[9] B.P. Leonard, A Stable and Accurate Convective Modeling Procedure Based on Quadratic Upstream Interpolation, Comput. *Method Appl. Mec. Eng.*, 23 (1979) 293–312.

[10] R.I. Issa, Solution of the implicitly discretised fluid flow equations by operator splitting, *J. Comput. Phys.*, 62 (1986) 40-65.

[11] H.T. P. Merkli, Thermo-acoustic effects in a resonance tube, *Journal of Fluid Mechanics*, 70 (1975) 161-177.

Please cite this article using:

A. Mohammadi and S. M. A. Alavi, "Investigation of Effective Parameters on a Thermal Load in a Thermo-Acoustic Refrigerator", *AUT J. Mech. Eng.*, 1(1) (2017) 49-54.

DOI: 10.22060/mej.2016.782